2019 IEEE 58th Conference on Decision and Control (CDC)
Palais des Congrès et des Expositions Nice Acropolis
Nice, France, December 11-13, 2019

Stop-and-go wave dissipation using accumulated controlled moving bottlenecks in multi-class CTM framework

Mladen Čičić[1] and Karl Henrik Johansson[1]

Abstract— **Stop-and-go waves on freeways are a well known problem that has typically been addressed using dynamic speed limits. As connected automated vehicles enter the roads, new approaches to traffic control are becoming available, since the control actions can now be communicated to these vehicles directly. It is therefore important to consider automated vehicles independently from the rest of the traffic, using traffic models with multiple vehicle classes. In this paper, we use a multi-class CTM to capture the interaction between the controlled vehicles and the background traffic. Exploiting the nonlinear nature of the model, we are able to first collect enough controlled vehicles into an area, and then use them to actuate the rest of the traffic by acting as a controlled moving bottleneck. In this way, we are able to dissipate stop-and-go waves quicker, improving the throughput and homogenizing the traffic. The effectiveness of the approach is demonstrated in simulations.**

I. Introduction

Controlling the traffic flow when the demand is close to road capacity is a very challenging and important task. Maintaining free flow with very high traffic density leads to an increased throughput, which reduces congestion levels and total travel time of all vehicles. However, this is a metastable situation, as small perturbations can often cause traffic breakdown and emergence of stop-and-go waves, also known as wide moving jams [1, 2] leading to a significant reduction in throughput. Furthermore, since vehicles need to decelerate or come to a full stop when entering the stop-and-go wave, their fuel consumption is increased, while the safety and comfort are decreased.

Resolving these stop-and-go waves enables the traffic to go return to a more desirable state. There have been several approaches dealing with this problem. In [3], a control law was proposed that uses variable speed limits (VSL). Although effective, this traffic control method requires variable message signs to communicate its control actions, reducing its flexibility and increasing its cost. With the introduction of new technologies, we expect to have the possibility to communicate control actions directly to the vehicles, either through an in-car advisory system in case of human drivers [4], or as commands to connected automated vehicles [5]. In [6], the control algorithm was combined with car-following control system, where connected automated vehicles adjust their behaviour based on nearby traffic conditions, leading to further improvements.

However, the performance of all these control algorithms suffers from low market penetration rate of connected automated vehicles, which is the situation that we are likely to have on the roads for quite some time [7]. In case variable message signs are not available at the location of interest, the only way of actuating VSL controls would be directly communicating it to the connected automated vehicles, which is equivalent to having an extremely low compliance rate. Therefore, there is an acute need to develop control approaches that can be used in this intermediate period when connected automated vehicles become available, but not in large numbers. Microscopic approaches, where we focus on the behaviour of individual vehicles and use automated vehicles to dissipate stop-and-go waves, have recently been proposed [8]. However, more detailed treatment of this problem in a macroscopic setting is still needed. To this end, there has been a decent amount of work on multi-class or multi-commodity macroscopic traffic flow models [9, 10]. Multi-class traffic models are typically inspired by the introduction of autonomous and connected vehicles, but can also provide a useful tool for capturing uncertainties in the flow model, or to precisely model the routes that vehicles take.

The problem we are addressing in this paper is stop-and-go wave dissipation using a small portion of connected automated vehicle that can be controlled directly from the infrastructure. We present a multi-class extension of the Cell Transmission model (CTM) and use it to model the interaction between connected automated vehicles and human-driven vehicles. We also propose an addition to the model that enables it to correctly model the behaviour of platoons and stop-and-go waves. Using this model, we derive a control law that uses the information about traffic density of each class along the road to first select a point at which we begin accumulating controlled vehicles, followed by accumulating enough vehicles to be able to influence the rest of the traffic, and finally controls the amassed moving bottleneck to dissipate the stop-and-go wave faster faster and increase the throughput of the road. In contrast to our previous work [11], where we required a heavy-duty vehicle to be at suitable position before using it as a controlled moving bottleneck, this enables us to choose where we create an accumulation of connected automated vehicles, offering us greater flexibility.

The outline of this paper is as follows. First, in Section II we present the multi-class CTM, and model platoons and

*The research leading to these results has received funding from the European Union's Horizon 2020 research and innovation programme under the Marie Skłodowska-Curie grant agreement No 674875, VINNOVA within the FFI program under contract 2014-06200, the Swedish Research Council, the Swedish Foundation for Strategic Research and Knut and Alice Wallenberg Foundation. The authors are affiliated with the Wallenberg AI, Autonomous Systems and Software Program (WASP).

[1]Division of Decision and Control Systems, KTH Royal Institute of Technology, Stockholm, Sweden Mladen Čičić: cicic@kth.se, Karl Henrik Johansson: kallej@kth.se

stop-and-go waves. Next, in Section III we devise a control strategy that for use in low penetration rate scenarios. We evaluate this control strategy in simulations in Section IV and finally conclude in Section V.

II. Model

A. The Multi-class CTM

The model that is presented and used in this work is a multi-class extension of the well-known CTM [12]. It is a modification of the model used in [13]. Let $\mathcal{K}$ be the set of vehicle classes $\kappa \in \mathcal{K}$. We express the contribution of all vehicle classes to the overall traffic density in terms of passenger car equivalents. The traffic density of vehicles of class κ in cell i at discrete time t will be denoted $\rho_i^\kappa(t)$. The model allows each of the classes to have a distinct free flow speed $U_i^\kappa(t)$ in every cell and at every time instant.

Assuming that the cells are of same length and that there are no on- or off-ramps, the evolution of cell traffic densities for each class is given by

$$\rho_i^\kappa(t+1) = \rho_i^\kappa(t) + \frac{T}{L}\left(q_{i-1}^\kappa(t) - q_i^\kappa(t)\right),$$

where T is the discretization step, $L = VT$ is the cell length, with V being the default free flow speed, and the traffic flow of each class is given by

$$q_i^\kappa(t) = \min(D_i^\kappa(t), S_{i+1}^\kappa(t)).$$

Due to shared road capacity, the demand and supply functions of each class $D_i^\kappa(t)$ and $S_i^\kappa(t)$ also depend on vehicles of other classes. We write the demand and supply functions

$$D_i^\kappa(t) = U_i^\kappa(t)\rho_i^\kappa(t)\min\left(1, \frac{F_i(t)}{\sum_{k\in\mathcal{K}} U_i^k(t)\rho_i^k(t)}\right),$$

$$S_i^\kappa(t) = \frac{\rho_{i-1}^\kappa(t)}{\rho_{i-1}(t)}\min\left(W_i(P_i - \rho_i(t)), V\sigma_i\right).$$

Here, σ_i and P_i the critical density and jam density of cell i, W_i the base congestion wave speed, function $F_i(t)$ models the cell capacity, and $\rho_i(t) = \sum_{\kappa\in\mathcal{K}}\rho_i^\kappa(t)$ is the aggregate traffic density. Where not stated otherwise, the critical density σ, jam density P and base congestion wave speed W will be equal for all cells, and $W = V\frac{\sigma}{P-\sigma}$, yielding a triangular fundamental diagram.

Out of many ways of modelling capacity drop in first-order traffic models [14], we chose to capture it as a linear reduction of capacity, [15]. Denoting by α the maximum capacity drop ratio under jam traffic density, we have

$$F_i(t) = \min\left(V\sigma_i, W_i\frac{\sigma_{i+1}}{\sigma_i}\left(P_i - (1-\alpha)\sigma_i - \alpha\rho_i(t)\right)\right). \quad (1)$$

Note that because of this phenomenon, the actual speed of the congestion wave will be different than W.

B. Platoons, Moving Bottlenecks and Stop-and-go Waves

Due to the discretization of the spatial coordinate, cell-based traffic models are often not adequate for capturing some traffic phenomena that have clear upstream and downstream boundaries that move in time, e.g. long vehicle platoons or stop-and-go waves. One way of dealing with this problem is to allow cell interfaces to move [16] and have these interfaces coincide with the boundaries. However, the information about the boundary position can often be encoded in traffic density of some classes. In this subsection, we describe how these phenomena can be correctly modelled in multi-class CTM.

Vehicle platoons consist of a number of vehicles driving together in a line as a single unit. If the platooning vehicles are connected and automated, this allows them to drive with shorter inter-vehicular distances, increasing the capacity of the road. In this work, we assume we will accumulate connected automated vehicles at certain points along the road, and model this accumulation as forming and joining a platoon. Let platooning vehicles belong to class a and background traffic to class b, and let the platoon move at speed $u_p \in [U_{\min}, U_{\max}]$. Note that simply setting $U_i^a(t) = u_p$ in cells where the platoon is would not be sufficient, since it would not maintain crisp boundaries of the platoon, as some vehicles would diffuse to the next cell. For example, for a one cell long platoon travelling at $u_p = V/2$, we have

$$\begin{aligned}
&\rho_i^a(0) = \rho_p, \quad \rho_{i+1}^a(0) = 0, \quad \rho_{i+2}^a(0) = 0,\\
&\rho_i^a(1) = \frac{\rho_p}{2}, \quad \rho_{i+1}^a(1) = \frac{\rho_p}{2}, \quad \rho_{i+2}^a(1) = 0,\\
&\rho_i^a(2) = \frac{\rho_p}{4}, \quad \rho_{i+1}^a(2) = \frac{\rho_p}{2}, \quad \rho_{i+2}^a(2) = \frac{\rho_p}{4},
\end{aligned}$$

whereas the correct behaviour would be

$$\rho_i^a(2) = 0, \quad \rho_{i+1}^a(2) = \rho_p, \quad \rho_{i+2}^a(2) = 0.$$

If we assume that platooning control maintains constant headways between the vehicles, so that the density of platooned vehicles is ρ_p, the densities of platooning vehicles in cells that contain the platoon would be

$$\rho_i^a(t) = \begin{cases} 0, & i < i_t^p(t) \vee i > i_h^p(t),\\ \rho_p\frac{x_t^p(t) - X_{i_t^p(t)+1}}{L}, & i = i_t^p(t),\\ \rho_p, & i_t^p(t) < i < i_h^p(t),\\ \rho_p\frac{x_h^p(t) - X_{i_h^p(t)}}{L}, & i = i_h^p(t), \end{cases} \quad (2)$$

where by $i_h^p(t)$ and $i_t^p(t)$ we denote the cells in which the platoon head and tail (downstream and upstream end) are at time t respectively, by $x_h^p(t)$ and $x_t^p(t)$ their exact positions, and by X_i the position of the upstream end of cell i. Since the platoon moves at speed u_p, $x_h^p(t+1) = x_h^p(t) + u_pT$ and $x_t^p(t+1) = x_t^p(t) + u_pT$, which the traffic densities $\rho_i^a(t+1)$ should follow. We may use the cell free flow speeds $U_i^a(t)$ to correctly model this behaviour by setting

$$U_i^a(t) = \begin{cases} V, & i < i_t^p(t),\\ \frac{V}{\rho_i^a(t)}\left(\rho_p - \frac{V - U_{i+1}^a(t)}{V}\rho_{i+1}^a(t)\right), & i_t^p(t) \le i < i_h^p(t),\\ V - (V - u_p)\frac{\rho_p}{\rho_{i_h}^a(t)}, & i = i_h^p(t),\\ 0, & i > i_h^p(t), \end{cases} \quad (3)$$

the traffic densities will both converge to (2) and evolve according to it, thus correctly modelling the behaviour of the platoon. Note that in case $\rho_i(t) = \rho_p$, $i_t^p(t) < i < i_h^p(t)$, we have $U_i^a(t) = u_p$, $i_t^p(t) < i < i_h^p(t)$. This approach only works if there are at least $n_{\min}^p = \rho_p L$ vehicles in a platoon.

Let the remainder of traffic consist of human-driven vehicles of class b, $U_i^b(t) = V$, and $\sigma_i = \sigma$. Under (3), the maximum class b traffic density flowing past the platoon will be $\rho^b_{i_p^h(t)+1}(t) = \sigma - \rho_p$. This is exactly the same result as we get for the maximum traffic density flowing past the moving bottleneck in the model described in [11] for $V_b = V$.

Similarly, in its basic form, the model cannot correctly represent the dynamics of stop-and-go waves and discharging traffic jams, even with capacity drop (1) included. For example, if a road is closed for some time and then reopened, discharging a traffic jam thus caused would evolve as

$$\begin{aligned}
&\rho_i(0) = P_i, && \rho_{i+1}(0) = 0,\\
&\rho_i(1) = P_i - (1-\alpha)\sigma_{i+1}, && \rho_{i+1}(1) = (1-\alpha)\sigma_{i+1},\\
&\rho_i(2) = \dots && \rho_{i+1}(2) = (1-\alpha)\sigma_{i+1}\left(1 + \frac{\alpha\sigma_{i+1}}{P_i - \sigma_i}\right),
\end{aligned}$$

whereas $\rho_i(2) = P_i - 2(1-\alpha)\sigma_{i+1}$, $\rho_{i+1}(2) = (1-\alpha)\sigma_{i+1}$ would be the correct behaviour.

In general, the discharge flow from a zone of density $\rho_c > \sigma_i$ will cause a zone of density

$$\rho_d = \frac{\sigma_{i+1}}{P_i - \sigma_i}\left(P_i - (1-\alpha)\sigma_i - \alpha\rho_c\right)$$

downstream. The wavefront separating the congestion from the free flow discharging from it propagates upstream,

$$\begin{aligned}
x_d(t+1) &= x_d(t) + \lambda_d T,\\
\lambda_d &= \frac{V\rho_d - W(P - \rho_c)}{\rho_d - \rho_c}.
\end{aligned} \tag{4}$$

Denoting by $i_c(t)$ and $i_d(t)$ the cells in which the upstream and downstream ends of the congestion zone are respectively, the correct aggregate traffic density profile is given by

$$\rho_i^*(t) = \begin{cases} \rho_c, & i_c(t) < i < i_d(t),\\ \rho_d + (\rho_c - \rho_d)\frac{x_d(t) - X_{i_d(t)}}{L}, & i = i_d(t),\\ \rho_d, & i > i_d(t). \end{cases}$$

This density profile can be achieved by setting appropriate free flow speeds for all vehicle classes, setting

$$U_{i_d}(t) = V\frac{\rho^*_{i+1}(t+1)}{\rho_i(t)} \tag{5}$$

for the downstream end, and then recursing

$$U_i(t) = \frac{V}{\rho_i(t)}\left(\rho_i^*(t+1) - \frac{V - U_{i+1}(t)}{V}\rho_{i+1}(t)\right) \tag{6}$$

for $i_c(t) \le i < i_d(t)$, same as in (3).

In summary, in this section we introduce the multi-class CTM for a road with no on- and off-ramps, as well as extensions that enable it to model platoons and stop-and-go waves. The model is intended for the situation when we have two vehicle classes, and can control one of them, but it is straightforward to extend it to cover different vehicle classes and other road networks.

III. Control

Next we use the developed model to derive a control law. Having detected a stop-and-go wave with downstream end at x_d, we can start attempting to dissipate it. We assume that there are two classes of vehicle, class a of automated vehicles that can be controlled from the infrastructure and class b of human-driven background traffic that cannot be directly controlled. Therefore, $U_i^a(t)$ is the control input that we can change in some range $0 \le U_{\min} \le U_i^a(t) \le U_{\max} \le V$, and we set $U_i^b(t) = V$ except where a different free flow speed is needed to properly model stop-and-go waves, where it is set by (5) and (6).

In case the control region is in free flow, $\rho_i(t) < \sigma$, we will have $q_i^\kappa(t) = U_i^\kappa(t)\rho_i^\kappa(t)$, and it is easy to show that ρ_i^b is not controllable by U_i^a. If class a vehicles only represent a very small portion of the traffic, the effect of solely controlling these vehicles in free flow will be very small; instead, we need to also indirectly control the background traffic by creating a controlled congestion. Therefore, the control we propose will consist of three phases:

1) selecting the initial point where we start accumulating controllable vehicles
2) collecting enough controllable vehicles so that they can affect the rest of traffic, and
3) using the collected controllable vehicles as a controlled moving bottleneck.

The overall control structure is outlined in Figure 1.

The simplest way of creating an accumulation of vehicles is to have a moving free flow speed gradient. Setting

$$U_i^a(t) = \begin{cases} U_{\max}, & i < i_p(t),\\ U_{\min}, & i \ge i_p(t), \end{cases}$$

where $X_{i_p(t)} < x_p(t) \le X_{i_p(t)+1}$ and x_p evolves as $x_p(t+1) = x_p(t) + u_p(t)T$, with $U_{\min} < u_p(t) < U_{\max}$ will cause class a vehicles to accumulate in cell $i_p(t)$ until they cause a congestion to emerge.

We are free to choose any point x_p^0 where we begin accumulating vehicles, and the process of calculating it is demonstrated in Figure 2. Denoting $\rho^\kappa(x,0) = \rho^\kappa_{\lfloor x/L \rfloor}(0)$ and setting $U_p^0 = U_{\max} = V$, the number of accumulated vehicles after time τ_p will be

$$n^a_{x_p^0, x_p'(\tau_p)}(0) = \int_{x_p^0}^{x_p'(\tau_p)} \rho^a(x, 0T)\mathrm{d}x,$$

where $x_p'(\tau_p) = x_p^0 + (U_{\max} - U_{\min})\tau_p$, i.e. all vehicles starting in $\left[x_p^0, x_p'(\tau_p)\right]$ will have accumulated in one cell after τ_p. Once more than $n^a_{p,\min} = \rho_p L$ vehicles are collected, where ρ_p is the goal platoon density, we can transition to the second phase of control and use the collected vehicles as a controlled moving bottleneck.

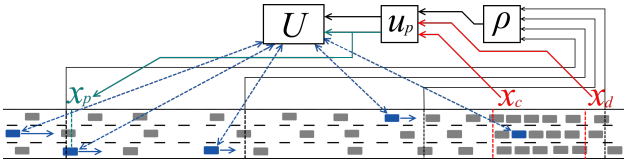

Fig. 1: Control loop sketch. We use the traffic density data and information about stop-and-go wave boundaries to calculate reference speeds for controlled vehicles. Vehicles upstream of $x_p(t)$ drive faster than those downstream, causing them to eventually accumulate at that point.

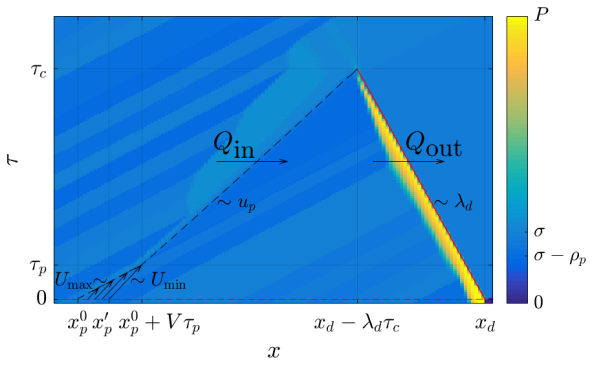

Fig. 2: Calculating x_p^0 given u_p. We calculate x_p^0 so that we accumulate enough vehicles after τ_p, continue moving the controlled bottleneck at speed u_p and reach the stop-and-go wave at time τ_c, exactly as it dissipates.

The flow out of the zone between x_p and x_d is

$$Q_{\text{out}} = (V - \lambda_d)\rho_d,$$

and the downstream end of the zone moves at speed λ_d given by (4). During the accumulation phase, the flow into the zone is zero with its upstream end moving at speed V, and assuming the controlled moving bottleneck moves at some speed U_p after the accumulation phase is complete, the flow into the zone is

$$Q_{\text{in}} = (V - U_p)(\sigma - \rho_p).$$

Therefore, we choose x_p^0 so that

$$n_{x_p^0, x_d^0}(0) = \int_{x_p^0}^{x_d^0} \rho(x, 0T)\mathrm{d}x = Q_{\text{out}}\tau_c - Q_{\text{in}}(\tau_c - \tau_p),$$
$$x_p^0 + V\tau_p + U_p(\tau_c - \tau_p) = x_d^0 + \lambda_d \tau_c,$$

where τ_p is determined by

$$n^a_{x_p^0, x_p'(\tau_p)}(0) = n^a_{p,\min}.$$

After collecting enough vehicles, we control them as if they were in a platoon with density ρ_p, as described in Section II-B. The control law is similar to the one from [11]. We now calculate the moving bottleneck speed $u_p(t)$ at each time instant so that it arrives at the stop-and-go wave exactly at the point when it dissipates,

$$u_p(t) = \frac{x_d(t) - x_p(t)}{\tau_c} + \lambda_d \tag{7}$$

where τ_c is calculated from

$$\tau_c = \frac{n_{x_p, x_d}(t) - (x_d(t) - x_p(t))(\sigma - \rho_p)}{(V - \lambda_d)(\rho_d - \sigma + \rho_p)}. \tag{8}$$

Substituting (8) into (7), we get

$$u_p(t) = \frac{V(\rho_d - \sigma + \rho_p) + \lambda_d(\bar{\rho}_{x_p, x_d}(t) - \rho_d)}{\bar{\rho}_{x_p, x_d}(t) - \sigma + \rho_p}, \tag{9}$$

where $\bar{\rho}_{x_p, x_d}(t)$ is the average traffic density between $x_p(t)$ and $x_d(t)$.

If any part of (9) is uncertain, it would be estimated from the data that is available. In particular, calculating $\bar{\rho}_{x_p, x_d}(t)$ might be challenging, since it requires information about traffic density in each cell. We may instead use the estimated average traffic density between $x_p(t)$ and $x_d(t)$,

$$\hat{\rho}_{x_p, x_d}(t) = \frac{\hat{n}_{x_p, x_d}(t)}{x_d(t) - x_p(t)} \tag{10}$$

where $\hat{n}_{x_p, x_d}(t)$ is the predicted number of vehicles between $x_p(t)$ and $x_d(t)$,

$$\begin{aligned}\hat{n}_{x_p, x_d}(t) = &\hat{n}_{x_p, x_d}(t-1) - (V - \lambda_d)\rho_d T + \dots \\ &\dots + (V - u_p(t-1))(\sigma - \rho_p)T,\end{aligned} \tag{11}$$

and (11) is initialized at time t_p when we transition from phase 1 to phase 2,

$$\hat{n}_{x_p, x_d}(t_p) = (x_c(t_p) - x_p(t_p))\hat{\rho} + (x_d(t_p) - x_c(t_p))\rho_c,$$

where $x_c(t)$ is the position of the upstream end of the stop-and-go wave, and $\hat{\rho}$ is the average overall traffic density, which can be calculated from the inflow to the network, or taken from historical data. Note that since we are not taking in new measurements of traffic density, nor of stop-and-go wave downstream and upstream ends, this variant essentially corresponds to feedforward control. Since we assume we can communicate with class a vehicles, and know their positions, we may use exact information about their density $\rho_i^a(t)$.

The control algorithm can further be adjusted by selecting the goal density $\rho_p \in [0, \sigma]$ and the moving bottleneck target speed $U_p \in [U_{\min}, U_{\max}]$. Physically, the most plausible choice is to select $\rho_p = \frac{\eta_l^p}{H_l}\sigma$, where H_l is the total number of lanes and η_l^p the number of lanes we want the moving bottleneck to occupy. By adjusting U_p, we influence at which point we begin assembling the vehicles, with a lower U_p leading to quicker dissipation of the stop-and-go wave, but with less room for adjustment in case there are some disturbances.

IV. Simulations

A. Simulation scenario

The parameters of the multi-class CTM model that were used are $V = 110$ km/h, $L = 0.5$ km, $T = L/V$, $\sigma = 60$ veh/km, $P = 240$ veh/km, $W = V\sigma/(P - \sigma)$, and $\alpha = 0.1$. The initial traffic density $\rho_i(0)$ is randomly generated, with every 5 adjacent cells taking a uniformly distributed value from $[0.8\sigma, \sigma]$. Similarly, the inflow into the first cell $q_0(t)$ is randomly generated in the same way, with every 5 samples taking a uniformly distributed value from $[0.8V\sigma, V\sigma]$. The ratio of connected automated vehicles in the initial traffic density, r_i^0, and in inflow, $r^q(t)$, also takes an uniformly distributed random value from $[0, 2\bar{r}]$, where $\bar{r}$ is the average ratio. For example, the initial density of class a vehicles in cell i is $\rho_i^a(0) = r_i^0\rho_i(0)$, while the initial density of class b is $\rho_i^b(0) = (1 - r_i^0)\rho_i(0)$, etc. We are considering 50 km of highway with no on- or off-ramps. At the beginning of each simulation, a stop-and-go wave is induced by fully closing the road for 2 minutes at a point close to the end of the considered stretch, after which we proceed with phase 1 of the described control law. Since the average inflow is equal to the discharge rate of the stop-and-go wave, it is

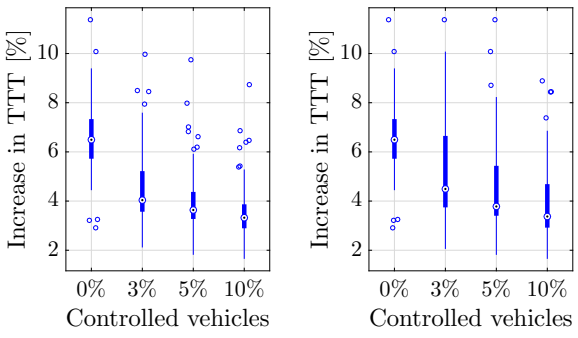

(a) Exact (b) Approximate

Fig. 3: Box plots of TTT change compared to the base case.

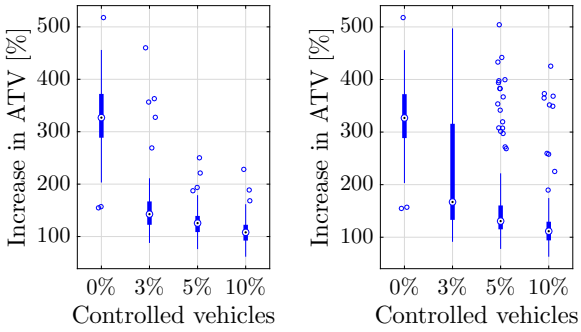

(a) Exact (b) Approximate

Fig. 4: Box plots of ATV change compared to the base case.

likely that unless some control action is applied, the wave will remain until the end of the simulation run.

We choose $\rho_d = \frac{\sigma}{3}$, i.e. the moving bottleneck will cover one third of the lanes, and use $U_p = 60\,\frac{\text{km}}{\text{h}}$, $U_{\min} = 50\,\frac{\text{km}}{\text{h}}$. Two different versions of the control law described in Section III will be compared. In the first one, we use exact information about the current traffic density when calculating (9), while in the second one we calculate $u_p(t)$ approximately, using estimated average density (10).

We will use *Total Travel Time* (TTT) [veh h], i.e. the total time all vehicles spend on the road,

$$\text{TTT} = \sum_{t=0}^{t_{\text{end}}} \sum_{i=1}^{N} \rho_i(t) TL,$$

as the traffic performance index to reflect the effect the control has on throughput of the road. In addition to throughput, we are also interested in how homogeneous the traffic conditions are. Therefore, we consider the *Average Total Variation* (ATV) of traffic density,

$$\text{ATV} = \sum_{t=0}^{t_{\text{end}}} \sum_{i=2}^{N} \frac{|\rho_i(t) - \rho_{i+1}(t)|}{t_{\text{end}}},$$

as a measure of traffic homogeneity, where lower ATV (higher homogeneity) is preferable to higher ATV (lower homogeneity). Essentially, the existence of a stop-and-go wave corresponds to high total variation of traffic density, so if the stop-and-go wave is dissipated quicker, we can expect the ATV to be lower.

B. Simulation results

We evaluate the two versions of the proposed control law in 100 simulation runs, with different average ratios of class a vehicles $\bar{r}^k$. The box plots of relative change of TTT and ATV, compared to the base case when no stop-and-go wave is induced, $\Delta\text{Index}_s^k = \frac{\text{Index}_s^k - \text{Index}_s^0}{\text{Index}_s^0}$, with s denoting the number of the simulation run, are shown in Figure 3 and Figure 4, respectively. The mean and median relative change of these indices are also given in Table I and Table II.

We can see that applying either version of the control law leads to improvements in both performance indices, even with penetration rates as low as 3%, with higher penetration rates leading to larger improvements, especially in case we use exact traffic density data. Approximate feedforward control is also more likely to fail to dissipate the stop-and-go wave, since it can underestimate the amount of vehicles between the controlled moving bottleneck and the downstream end of the stop-and-go wave, as witnessed by a higher spread or number of outliers in Figures 3 and 4.

To further illustrate the influence the ratio of controlled vehicles has, as well as highlight the difference in performance of the two control versions, in Figure 5 we compare the execution of one simulation run for different penetration rates and control law versions. In Figure 5a and 5b we compare the exact and the approximate feedforward control laws under penetration rate of $\bar{r} = 5\%$. In the latter case, the speed of the controlled moving bottleneck is too high due to underestimating the traffic volume, causing it to arrive at the stop-and-go too early and fail to dissipate it.

Additionally, by comparing Figure 5a and Figure 5c, we see the benefit of having a higher penetration rate of connected automated vehicles. In case $\bar{r} = 10\%$, we are both able to start collecting the vehicles closer to the stop-and-go wave, and finish collecting enough of them much quicker than in case $\bar{r} = 5\%$. This allows us to dissipate the stop-and-go wave quicker, leading to improvement in both performance indices.

TABLE I: Mean and median change in TTT compared to the base case with no stop-and-go wave formed.

$\bar{r}^k$ [%]	exact		approximate	
	mean	median	mean	median
0%	6.6%	6.49%	6.6%	6.49%
3%	4.51%	4.04%	5.22%	4.49%
5%	3.99%	3.64%	4.49%	3.78%
10%	3.58%	3.32%	3.82%	3.37%

TABLE II: Mean and median change in ATV compared to the base case with no stop-and-go wave formed.

$\bar{r}^k$ [%]	exact		approximate	
	mean	median	mean	median
0%	331.13%	326.87%	331.13%	326.87%
3%	153.46%	142.76%	216.99%	167.01%
5%	127.73%	125.63%	169.84%	130.67%
10%	109.92%	107.99%	129.88%	111.45%

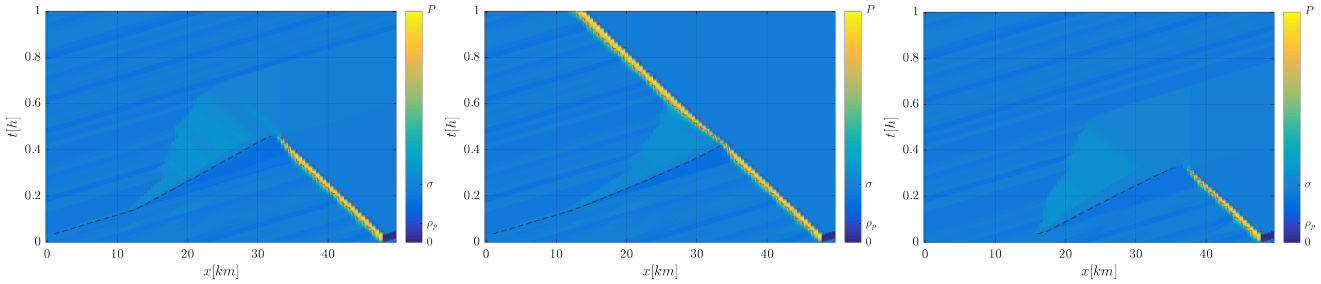

(a) Exact, 5% (b) Approximate, 5% (c) Exact, 10%

Fig. 5: One example simulation run for different ratios of controlled vehicles and version of the control algorithm.

V. Conclusion

In this paper we deal with the problem of dissipating stop-and-go waves by use of a small portion of vehicles that we can control directly. We first accumulate enough of controlled vehicles, increasing their share in the overall traffic at some position, and once enough vehicles are gathered, use them to restrict the traffic flow as a controlled moving bottleneck, effectively starving the congestion of inflow and causing it to dissipate sooner. Since the outflow from a stop-and-go wave is lower than road capacity, this causes the throughput to increase. The control law is evaluated using Total Travel Time and Average Total Variation as performance indices, and shown to lead to improvement in both. We also propose an approximate feedforward control law that only uses average or historical information about traffic densities, resulting in somewhat diminished improvements in TTT and ATV.

There are many other traffic control problems that can be tackled using the presented multi-class CTM and similar control approaches. For example, vehicle trajectory optimization at a signalized intersection or bottleneck decongestion are typically studied in microscopic traffic model setting, which necessitates simulating and considering a large number of individual vehicles. However, the solutions often lead to emergent behaviours with clear spatio-temporal patterns, which may be captured by macroscopic models. By adapting these solutions, we might be able to achieve similar results by applying a more general control action to all vehicles within a spatio-temporal region, instead of calculating separate control for all individual vehicles, thus greatly improving the tractability of the problem.

References

[1] B. S. Kerner, "Experimental features of the emergence of moving jams in free traffic flow," *Journal of Physics A: Mathematical and general*, vol. 33, no. 26, p. L221, 2000.

[2] Y. Sugiyama, M. Fukui, M. Kikuchi, K. Hasebe, A. Nakayama, K. Nishinari, S.-i. Tadaki, and S. Yukawa, "Traffic jams without bottlenecks–experimental evidence for the physical mechanism of the formation of a jam," *New journal of physics*, vol. 10, no. 3, p. 033001, 2008.

[3] A. Hegyi, S. Hoogendoorn, M. Schreuder, H. Stoelhorst, and F. Viti, "SPECIALIST: A dynamic speed limit control algorithm based on shock wave theory," in *11th IEEE International Conference on Intelligent Transportation Systems*, 2008, pp. 827–832.

[4] W. J. Schakel and B. Van Arem, "Improving traffic flow efficiency by in-car advice on lane, speed, and headway," *IEEE Transactions on Intelligent Transportation Systems*, vol. 15, no. 4, pp. 1597–1606, 2014.

[5] P. Ioannou, Y. Wang, and H. Chang, "Integrated roadway/adaptive cruise control system: Safety, performance, environmental and near term deployment considerations," *California PATH Program, Institute of Transportation Studies, University of California at Berkeley*, 2007.

[6] M. Wang, W. Daamen, S. P. Hoogendoorn, and B. Van Arem, "Connected variable speed limits control and car-following control with vehicle-infrastructure communication to resolve stop-and-go waves," *Journal of Intelligent Transportation Systems*, vol. 20, no. 6, pp. 559–572, 2016.

[7] T. Litman, *Autonomous vehicle implementation predictions*. Victoria Transport Policy Institute Victoria, Canada, 2017.

[8] R. E. Stern, S. Cui, M. L. D. Monache, R. Bhadani, M. Bunting, M. Churchill, N. Hamilton, R. Haulcy, H. Pohlmann, F. Wu, B. Piccoli, B. Seibold, J. Sprinkle, and D. B. Work, "Dissipation of stop-and-go waves via control of autonomous vehicles: Field experiments," *Transportation Research Part C: Emerging Technologies*, vol. 89, pp. 205 – 221, 2018.

[9] M. W. Levin and S. D. Boyles, "A multiclass cell transmission model for shared human and autonomous vehicle roads," *Transportation Research Part C: Emerging Technologies*, vol. 62, pp. 103–116, 2016.

[10] J. Van Lint, S. Hoogendoorn, and M. Schreuder, "Fastlane: New multiclass first-order traffic flow model," *Transportation Research Record: Journal of the Transportation Research Board*, no. 2088, pp. 177–187, 2008.

[11] M. Čičić and K. H. Johansson, "Traffic regulation via individually controlled automated vehicles: a cell transmission model approach," in *21st IEEE International Conference on Intelligent Transportation Systems*, Maui, US, 2018.

[12] C. F. Daganzo, "The cell transmission model: A dynamic representation of highway traffic consistent with the hydrodynamic theory," *Transportation Research Part B: Methodological*, vol. 28, no. 4, pp. 269–287, 1994.

[13] G. Piacentini, M. Čičić, A. Ferrara, and K. H. Johansson, "VACS equipped vehicles for congestion dissipation in multiclass CTM framework," in *European Control Conference*, 2019.

[14] M. Kontorinaki, A. Spiliopoulou, C. Roncoli, and M. Papageorgiou, "First-order traffic flow models incorporating capacity drop: Overview and real-data validation," *Transportation Research Part B: Methodological*, vol. 106, pp. 52–75, 2017.

[15] Y. Han, Y. Yuan, A. Hegyi, and S. P. Hoogendoorn, "New extended discrete first-order model to reproduce propagation of jam waves," *Transportation Research Record: Journal of the Transportation Research Board*, no. 2560, pp. 108–118, 2016.

[16] C. C. de Wit and A. Ferrara, "A variable-length cell road traffic model: application to ring road speed limit optimization," in *55th IEEE Conference on Decision and Control*, 2016.